PCCP

Accepted Manuscript

This is an *Accepted Manuscript*, which has been through the Royal Society of Chemistry peer review process and has been accepted for publication.

Accepted Manuscripts are published online shortly after acceptance, before technical editing, formatting and proof reading. Using this free service, authors can make their results available to the community, in citable form, before we publish the edited article. We will replace this *Accepted Manuscript* with the edited and formatted *Advance Article* as soon as it is available.

You can find more information about *Accepted Manuscripts* in the Information for Authors.

Please note that technical editing may introduce minor changes to the text and/or graphics, which may alter content. The journal's standard Terms & Conditions and the Ethical guidelines still apply. In no event shall the Royal Society of Chemistry be held responsible for any errors or omissions in this *Accepted Manuscript* or any consequences arising from the use of any information it contains.

ROYAL SOCIETY OF CHEMISTRY

www.rsc.org/pccp

Pore Orientation Effects on the Kinetics of Mesostructure Loss in Surfactant Templated Titania Thin Films

Saikat Das[a,†], Suraj Nagpure[a], Ravinder K. Garlapalli[a,‡], Qingliu Wu[b], Syed Z. Islam[a], Joseph Strzalka[c], Stephen E. Rankin[a,*]

[a] *Chemical & Materials Engineering Department, University of Kentucky, Lexington, KY*
[b] *Chemical Sciences and Engineering Division, Argonne National Laboratory, Argonne, IL*
[c] *Advanced Photon Source, Argonne National Laboratory, Argonne, IL*

* Author to whom correspondence should be addressed. E-mail: srankin@engr.uky.edu. Tel: +1-859-257-9799

† Current address: Department of Civil and Environmental Engineering, University of Michigan, Ann Arbor, MI

‡ Current address: Chemical and Biomolecular Engineering Department, Ohio University, Athens, OH

Physical Chemistry Chemical Physics Accepted Manuscript

Abstract

The mesostructure loss kinetics are measured as a function of the orientation of micelles in 2D hexagonal close packed (HCP) columnar mesostructured titania thin films using *in situ* grazing incidence small angle x-ray scattering (GISAXS). Complementary supporting information is provided by *ex situ* scanning electron microscopy. Pluronic surfactant P123 acts as the template to synthesize HCP structured titania thin films. When the glass substrates are modified with crosslinked P123, the micelles of the HCP mesophase align orthogonal to the films, whereas a mix of parallel and orthogonal alignment is found on unmodified glass. The rate of mesostructure loss of orthogonally oriented (o-HCP) thin films (~60 nm thickness) prepared on modified substrate is consistently found to be less by a factor of 2.5±0.35 than that measured for mixed orientation HCP films on unmodified substrates. The activation energy for mesostructure loss is only slightly greater for films on modified glass (155±25 kJ/mol) than on unmodified (128 kJ/mol), which implies that the rate difference stems a greater activation entropy for mesostructure loss in o-HCP titania films. Nearly perfect orthogonal orientation of micelles on modified surfaces contributes to the lower rate of mesostructure loss by supporting the anisotropic stresses that develop within the films during annealing due to continuous curing, sintering and crystallization into the anatase phase during high temperature calcination (>450 °C). Because the film thickness dictates the propagation of orientation throughout the films and the degree of confinement, thicker (~250 nm) films cast onto P123-modified substrates have a much lower activation energy for mesostructure loss (89±27 kJ/mol) due to the mix of orientations found in the films. Thus, this kinetic study shows that thin P123-templated o-HCP titania films are not only better able to achieve good orthogonal alignment of

Physical Chemistry Chemical Physics Accepted Manuscript

the mesophase relative to thicker films or films on unmodified substrates, but that alignment of the mesophase in the films stabilizes the mesophase against thermally-induced mesostructure loss.

1. Introduction

Templated nanoporous titania thin films, prepared via evaporation-induced self-assembly (EISA),[1-3] have attracted scientific interest for the last two decades in numerous applications such as photovoltaics,[4-6] electronic devices,[7, 8] photocatalysis [9-11] and sensors.[12, 13] The well-ordered uniform titania pores, created after removal of a templating agent (surfactant[14] or block copolymer[15]), offer unique physicochemical properties such as high surface area, affinity towards certain ligands, and electronic conductivity, that makes mesoporous titania thin films a perfect candidate for the applications mentioned above.[16, 17] By varying the ratio of titania precursor to templating agent it is possible to generate titania films with a wide variety of well-ordered mesostructures including lamellar, cubic and 2D hexagonally close packed (HCP).[18-24] Among these phases, 2D HCP cylindrical pores are of particular interest because they provide well defined short diffusion paths for reactants and charge carriers, ideal for photoelectrochemistry or introducing wires for reaction with a contacting phase.[25-27] However, a major barrier to the application of 2D HCP mesoporous titania is that the pores of the structure typically align parallel to the coating substrate due to preferential interactions between hydrophilic substrates (such as glass, ITO or silicon wafers) and the polar components of the film (the titania precursor and polar parts of templating agent).[28] Parallel pores are only poorly accessible to reactants (perhaps via defects in the HCP structure), and thus are not usable in many of the applications of interest for titania.[29]

Physical Chemistry Chemical Physics Accepted Manuscript

The HCP pore orientation problem can be overcome by a variety of approaches using fields, confinement, and surface modification techniques that make the substrate neutral with respect to the polar and nonpolar parts of the templating agent.[30] Koganti et al. have shown for P123 templated titania thin films that it is possible to produce HCP mesopores aligned orthogonal to the substrate by first using a crosslinked layer of a surface modifier such as poly(ethylene oxide-r-propylene oxide) copolymer or P123 itself, and then by sandwiching the films.[31, 32] The resulting films have accessible uniform cylindrical nanopores tilted so that they are accessible, and thus usable for applications analogous to anodized titanium films that call for a photochemically active titania matrix.[33-35] The advantage of the surfactant templating approach, however, is that it allows for smaller pores to be produced more readily than anodization, and as a coating process, it also can be scaled up for large-area production and adapted for a variety of substrates and interfacial chemistries.

Along with the ordered mesostructure it is necessary to control titania crystallinity for (photo)electrochemical applications as it plays a significant role in tuning the band gap and charge carrier mobility.[36-38] Sol-gel derived titania films generally are amorphous after formation and crystallinity emerges with the formation of anatase during heat treatment above 400 °C.[39, 40] Crystallization of titania by heat treatment comes with the potential sacrifice of mesostructural order due to the large amount of atomic movement during crystallization.[41, 42] The tradeoff between maintaining mesopore structure and developing crystallinity during thermal treatment is a well-known challenge that has been addressed in prior studies. Kirsch et al. used a combination of wide- and small- angle x-ray scattering to measure activation energies for anatase formation vs. mesostructure loss in P123-templated $Im\bar{3}m$ cubic titania films.

Physical Chemistry Chemical Physics Accepted Manuscript

Because they observed a greater activation energy for crystallization, they recommended rapid, high temperature thermal treatments to promote crystallization with minimal mesostructure loss.[43] Bass et al. studied the effects of mesostructure symmetry and concluded that mesostructural order stabilizes films, while disorder in the mesophase make the films crystallize similar to nonporous TiO_2 films,[44] which is also consistent with the report of Carreon et al.[45]

A prior study by Das et al. showed that titania films with orthogonally oriented HCP (o-HCP) pores generated by sandwiching films between two modified substrate have better thermal stability than films with mixed pore orientation prepared from the same coating solution on a single modified substrate.[46] The enhanced stability was attributed to differences in the ability of the o-HCP structure to withstand anisotropic stress during curing and a change in the mode of anatase nucleation. However, there are some limitations of using the sandwiching approach to controlling mesostructured orientation. It is a manual technique which is susceptible to variability in surface homogeneity, pressure during sandwiching, and time between film coating and sandwiching. Also this technique may not be suitable for some applications where the top surface of the films needs to be modified just after coating.[47, 48] Sandwiching also introduces the possibility that the differences observed in thermal stability were caused by a surface phenomenon such as heterogeneous nucleation of the anatase phase. To overcome these limitations, Koganti et al. showed that the orthogonally oriented pores can also be created using only one modified substrate below a critical thickness (~100 nm).[31]

Here we present a detailed study of the kinetics of the mesostructural transformation of thin (<100 nm thick) titania films using *in situ* grazing incidence small angle x-ray scattering (GISAXS) complemented by *ex situ* scanning electron microscopy (SEM). Transformation kinetics

Physical Chemistry Chemical Physics Accepted Manuscript

are studied as a function of pore orientation induced by modifying the surface or by changing the film thickness. The *in situ* GISAXS data are gathered with sufficient temporal resolution to allow kinetics to be followed and are modeled using the Avrami equation at each temperature. Arrhenius temperature dependence is assumed to determine the activation energy for mesostructural deterioration for each case. The hypothesis to be tested is that thin films (~60 nm thick) prepared on a modified glass substrate with o-HCP structure have higher activation energy or entropy for mesostructure loss than films with parallel or mixed HCP pores on unmodified substrates, which explains their greater thermal stability. A second part of the study will use thicker (~250 nm thick) films to address the effects of film thickness on the propagation of orientation throughout the films. It is expected that thicker films will have lower activation energy for mesostructure deterioration compared to thinner films on both unmodified and modified substrates, due to the mix of HCP orientations in these films. The study also includes measurements of the effects of temperature ramp rate on mesostructure transformation of titania thin films to search for possible optimal conditions for heating.

2. Experimental section

Surfactant-templated titania thin films were prepared based on the procedures of Koganti et al.[31] Prior to depositing any material, plain borosilicate glass slides were cleaned with a NoChromix glass cleaning solution (Godax Laboratories, Inc.) prepared according to the package instructions. Cleaned glass slides were then modified by dip coating with an acetone solution containing equimolar amounts (0.415 mM) of Pluronic surfactant P123 (poly(ethylene glycol)-block-poly(propylene glycol)-block-poly(ethylene glycol) with M_n ~ 5800, Sigma-Aldrich) and 1,6-diisocyanatohexane (98%, Sigma Aldrich). To this solution, a single drop of glycerol was

Physical Chemistry Chemical Physics Accepted Manuscript

added to serve as a cross-linker so that the films would be stable. The slides with a modifying coating were aged at 120 °C overnight to drive the cross-linking reaction to completion. Titania sols were prepared by adding 2.1 g of titanium ethoxide (technical grade, Sigma Aldrich) to 1.53 g of concentrated HCl (36 wt%, EMD Chemicals), stirring for 10 min and adding 0.65 g P123 dissolved in 32 g or 6 g of ethanol (200 Proof, Decon Laboratories) for thin or thick films, respectively. Films were dip coated at a 7.6 cm/min withdrawal rate from the titania sol onto P123-modified or unmodified glass slides and then were aged in a humid environment (RH 66%) in a refrigerator (4 °C) for 2 hr. The humid environment was achieved by placing two small beakers of possasium nitrate-saturated aqueous solution in a closed box along with the slides to allow vapor-phase equilibration of water.

In situ GISAXS experiments were done at the Advanced Photon Source at Argonne National Laboratory on beamline 8-ID-E[49] using a wave length of 1.687 Å and a sample-detector distance of 1397.7 mm. Aged samples were placed on a sample holder which was connected with heating coils and then heated to a desired final calcination temperature with different ramp rates. After reaching the final calcination temperature, all samples were kept at that temperature during *in situ* GISAXS measurements. The heating device used was a stainless steel block with a temperature controller. The thermocouple used for temperature control was placed on the titania film as close as possible to the sampled area without interfering with the scattering. A GISAXS pattern was collected at room temperature before heat was turned on and again after the final temperature was attained, at which point the sample was realigned. *In situ* data were collected with a Pilatus 1M pixel array detector using a 1 sec exposure time. Images were corrected for detector nonuniformity and converted to q-space using the GIXSGUI

Physical Chemistry Chemical Physics Accepted Manuscript

package for Matlab.[50] All images shown are 1 second exposures displayed on the same logarithmic intensity scale.

To complement the GISAXS measurements, the mesoporous structures of selected titania films were examined using a Hitachi S-900 Scanning electron microscope instrument at 6 kV voltage. The samples were prepared for SEM by cutting a small piece of the titania film-coated substrate and attaching it onto a SEM stub with carbon tape. A coating of colloidal graphite (isopropanol base) was applied to the sample edges to increase conductivity by creating an electrical contact between the top surface of the film and the stub.

3. Results and Discussion

Fig. 1 shows SEM images of P123 templated titania thin films (60 nm thick after calcination at 500 °C as measured by ellipsometry, prepared using 32 g of ethanol) on both an unmodified borosilicate glass substrate and one modified with crosslinked P123. For titania films on unmodified substrate, HCP pores were expected to be oriented parallel to the substrate due to preferential interactions of the headgroups of the templating agent with the hydrophilic substrate.[31] Instead, Fig. 1a shows that some degree of orthogonal orientation of pores was present in films on unmodified substrates, indicated by pore openings present in the SEM image after calcination. Partial orthogonal alignment of HCP titania composite films on unmodified slides was also found in an *in situ* GISAXS study of aging in these films,[51] and may be a result of decreased segregation between poly(ethylene oxide) [PEO] and poly(propylene oxide) [PPO] blocks during aging at low temperature. The fragments of material on top of the film in Fig. 1a may be collapsed sections of the top layer of film which were initially oriented parallel to the substrate but whose structure collapsed during heating.[46] In contrast, Fig. 1b

Physical Chemistry Chemical Physics Accepted Manuscript

shows the 2D HCP pattern of well-ordered pores with perfectly orthogonal orientation on a P123-modified substrate. The average distance between pores in the SEM images is estimated to be approximately 14-15 nm for both types of films, so the main difference between them is the degree of orthogonal orientation of the HCP mesophase. The preservation of o-HCP domains in the films after calcination at 500 °C is consistent with the previous study of Das et al. where the contrast in orientation was achieved by sandwiching thicker films.[46]

To better understand the initial structure of the films, Fig. 2 compares the GISAXS patterns of mesostructured titania / P123 composite films on both unmodified and P123-modified substrates at room temperature after aging but before heating. The films were aligned horizontal relative to the incident x-ray beam. Fig. 2a shows a combination of intense out-of-plane and in-plane diffraction spots in the GISAXS pattern, as well as an isotropic ring due to randomly oriented domains. Out-of-plane spots were indexed to a distorted 2D HCP mesophase parallel to the substrate with rectangular symmetry (space group C2mm),[46, 52] and the in-plane spots were indexed to an orthogonally oriented 2D HCP phase. Unit cell parameter for the rectangular pattern are a = 14 nm and b = 17.3 nm. The ratio b/a = 1.4, which represent 19% contraction normal to the plane of the film compared to an ideal hexagonal structure (which would have b/a = 1.73). The unit cell parameter for the vertically aligned hexagonal spots is a = 16.8 nm. The overall pattern is consistent with a mixed orientation HCP structure. A comparison of calculated and measured d-spacing values based on this indexing is shown in Supporting Information Fig. S1. In the case of a titania film on P123-modified substrate (Fig. 2b), orthogonally oriented HCP domains predominate, as indicated by the two intense in-plane vertical Bragg rods located on both sides of the beam stop and a faint isotropic ring and even

Physical Chemistry Chemical Physics Accepted Manuscript

fainter traces of the out-of-plane spots due to remnants of randomly oriented domains or mesophase oriented parallel to the substrate. This is consistent with the SEM image in Fig. 1b obtained after calcination of this structure. The Bragg rod intensity appears weak because of the high intensity of the diffuse scattering from the x-ray beam above the beamstop. A direct comparison of the fraction of orthogonal mesophase is not possible because no perfectly oriented standards are available, but comparing GISAXS patterns before calcination for another pair of films (Supporting Information Fig. S2) shows that more intense vertical rods are present on the unmodified substrate consistent with a larger fraction of o-HCP domains. Supporting Information Fig. S3 compares linecuts extracted from GISAXS images before calcination from q_z = 0.05-0.06 $Å^{-1}$ and shows significantly greater intensity of in-plane diffraction from the o-HCP structure in the film prepared on a modified substrate.

To determine how the degree of orthogonal alignment affects mesostructure evolution during heating, films on P123-modified and unmodified substrates were subjected to heating. Thermal expansion of the materials necessitates realignment of the sample and precluded collection of GISAXS data during the ramp from room temperature to the final temperature, but data collection began as soon as possible after realignment upon reaching the final temperature. Fig. 3 shows representative examples of the GISAXS patterns from titania films on both unmodified and modified substrates just after reaching a final calcination temperature of 600 °C and realigning the sample. For a final calcination temperature below 600 °C, no significant change in the intensity of the diffraction spots was seen after holding the titania films for 60 minutes (e.g. at 550 °C, Supporting Information Fig. S4). During the heating of the templated titania films the polymer was expected to be oxidized and completely removed at

Physical Chemistry Chemical Physics Accepted Manuscript

350 °C [46] thus leaving behind a porous titania structure. It is evident from Fig. 3 that both films on unmodified substrate (Fig. 3a) and on modified substrate (Fig. 3b) have lost some mesotructural order over the course of ramping to an elevated temperature. In Fig. 3a, there are no out of plane spots, indicating total loss of domains with parallel (distorted) HCP orientation. Although vertical rods can be seen in Fig. 3a, they have lost significant intensity and have become broader compared to the initial GISAXS pattern at room temperature (Fig 2a). All of these features indicate that for titania films on unmodified substrates, the domains of parallel HCP pores are much more susceptible to thermal deterioration than the orthogonally oriented domains. To make sure that the deterioration described in the previous measurements was only due to thermal treatment and not due to beam damage, the GISAXS pattern of a separate spot was measured (data not shown) after the completion of the annealing process but it showed similar loss of mesostructural order compare to previously examined spot. This result confirms that the mesostructural loss was only due to thermal treatment.

The order of the orthogonally oriented pores in films on modified substrates also starts to deteriorate and the pore size distribution may become broader, as indicated by broadening and loss of intensity of the vertical rods in Fig. 3b, compare to the initial condition at room temperature in Fig. 2b. However, the change is less than for the unmodified substrates (Fig. 3a). This loss of mesostructural order is caused by curing, diffusion and sintering during heating, and possibly by anisotropic stress developed due to crystallization of titania in the pore walls, starting above ~450 °C.[46]

Physical Chemistry Chemical Physics Accepted Manuscript

While they have some similarity just after reaching 600 °C, the GISAXS patterns of P123-templated titania films on unmodified and modified substrates differ dramatically after holding the samples at this temperature for 60 min (Fig. 4). The titania film on unmodified substrate (Fig. 4a) has a diffuse pattern centered around the Yoneda band with only faint vertical rods, indicating nearly complete loss of long-range mesostructural order. In contrast, titania films on modified substrates not only retained a significant amount of mesotructural order for the initial 60 min measurement (indicated by vertical rods in in Fig. 4b), but for at least another 30 min during the GISAXS (data not shown). SEM imaging was performed using the same samples as those used for GISAXS experiments after calcination at 600 °C to observe the pore structure. As Fig. 5 shows, the titania film on the unmodified substrate (Fig. 5a) has some accessible pores but has lost its long-range mesostructural order completely after 60 min at 600 °C, consistent with the GISAXS pattern (Fig. 4a). In contrast, the titania film on modified substrate (Fig. 5b) still retains some long range mesopore order even after 90 min at 600 °C. Wide-angle x-ray scattering after calcination at 600 °C (Supporting Information Fig. S5) shows the presence of anatase with the most intense ring at q =1.8 $Å^{-1}$ corresponding to the (101) plane, but its intensity is not proportional to the degree of mesostructure loss. Instead, the o-HCP structure prepared on a modified slide exhibits greater (101) diffracted intensity, which suggests that crystallization and mesostructure loss occur simultaneously but that they can be controlled independently, as suggested by Kirsch et al.[43]

To quantify and compare the stability of the mesostructural order in the films on both unmodified and modified substrates, 2D GISAXS data were taken in 5 min intervals and a slice of each pattern was taken at q_z = (0.06-0.07) $Å^{-1}$ after reaching the final calcination

Physical Chemistry Chemical Physics Accepted Manuscript

temperature. While it is not in the Yoneda band, this q_z range was chosen because it is quite sensitive to the presence and intensity of Bragg rods due the o-HCP structure. The area under the vertical rod, the orthogonal (100) peak, was determined after baseline correction and normalized by the peak area just after reaching the final calcination temperature. Fig. 6 shows the time evolution of the normalized area under the (100) peak after reaching 600 °C for titania films on both unmodified and modified substrates. While both films show deterioration in the intensity of this peak in contrast to calcination below 600 °C (see Supporting Information Fig. S6), the film on modified substrate better retains its long range order compared to the film on unmodified substrate. Consistent with the 2D patterns in Fig. 4, the normalized intensity for the film on a modified substrate is almost 5 times higher than for the film on an unmodified substrate after the 60 min of holding at 600 °C.

Insight into the mechanism of the thermal transformation was gained by applying the Avrami equation. The Avrami equation is often used to analyze phase transformation processes involving continuous nucleation and growth or loss of a phase.[53, 54] In our case we observe continuous loss of the mesostructural order with calcination time so that the Avrami equation can be applied in a manner similar to Kirsch et al. who studied the competition between crystallization and mesostructure loss in mesoporous TiO_2 films.[43] The Avrami equation is given by Eq. 1:

$$-ln(1-\alpha) = (kt)^n \quad (1)$$

where α = the fraction of mesostructural order remaining, t = time, k = the rate coefficient of mesostructural deterioration and n = transformation propagation parameter.

Eq. 1 can further be linearized to give Eq 2:

Physical Chemistry Chemical Physics Accepted Manuscript

$$ln\big(-ln(1-\alpha)\big) = n * ln(t) + n * ln(k) \quad (2)$$

Isothermal evolution studies of mesostructural deterioration of titania films on both unmodified and modified substrate were done for three different temperatures (600 °C, 625 °C and 650 °C) and the *in situ* data were fit by linear regression using Eq. 2. Fig. 7 shows the fitting at each temperature for each sample. The linearized form of the Avrami equation fit all isothermal data reasonably well and can be further used to determine the kinetic parameters associated with these mesostructural deterioration processes. The values of *n* and *k* at each temperature are summarized in Table 1. For all experiments, the value of *n* associated with mesostructure loss is between 0.63 and 1.1, which is consistent with a one dimensional diffusion controlled mechanism for the thermal transformation of these titania films. [55, 56] This suggests that loss of order occurs due to diffusion along the walls of the material in a preferred direction due to the HCP structure. Increasing rate coefficient (*k*) values with temperature for films on both unmodified and modified substrates in Table 1 indicate an activated process for loss of order.

The effect of orientation on the activation energy for mesostructure loss was determined using the linearized Arrhenius equation (Eq. 3):

$$ln\, k = ln\, A - E_a/(R * T) \quad (3)$$

where *A* = a pre-exponential factor, E_a = activation energy for mesostructural deterioration, *T* = absolute temperature and *R* = universal gas constant.

Fig. 8 shows plots of ln(*k*) vs 1/*T* for the titania films, from which activation energies of 126±100 kJ/mol for films on unmodified substrates and 155±25 kJ/mol for films on P123-modified substrates were determined. This activation energy is associated with the

Physical Chemistry Chemical Physics Accepted Manuscript

deterioration of the orthogonal component of the HCP structure for titania films on both unmodified and modified substrate, as the parallel domain is already absent above 400 °C.[46] These activation energy values are comparable with the activation energy described in the literature for the deterioration of titania films with cubic mesostructure (140 KJ/mol).[43] The large standard error associated with the activation energy for the films on unmodified substrate is due to the large deviation in the measurement at 625 °C compared to trend measured at the other temperatures. This is point is most likely an outlier because its rate coefficient is lower than at 600 °C. Unfortunately, due to limitations in beam time available, the measurement could not be replicated, so the standard error reported includes that measurement. If it is not included, the calculated activation energy is 128 kJ/mol although no uncertainty can be calculated with only two points. While the outlier does not allow a strict statistical comparison, a slightly higher activation energy for films on the modified substrate is apparent, which means that the orthogonally oriented domains of titania films on modified substrates are more thermally stable than the orthogonal domains of films on unmodified substrates. The pre-exponential factor for mesostructure loss in thin films on modified slides is $A = 4.4 \times 10^7$ min^{-1} ± 19%, which indicates a greater entropy of activation than for the unmodified slides ($A = 3.0 \times 10^6$ min^{-1}) assuming that the films have the same frequency factor for this process.

The reason for the difference in stability may be that the density of bending defects, or tortuosity associated with the orthogonal component, is higher for films on unmodified substrates (which start with a significant fraction of parallel domains) than the more uniform orthogonal domains on the modified substrate. The heterogeneity of the domains of films on unmodified substrates would be expected to introduce more defects to concentrate stress and

Physical Chemistry Chemical Physics Accepted Manuscript

nucleate loss of order in the orthogonal domains, and would also be less resistant to anisotropic stress than films on modified substrates with more uniform orthogonal domains and a well-defined path for diffusion of atoms during crystallization and curing.

The effects of film thickness on the thermal stability of this system were also studied for P123-templated titania films on P123 modified substrates. The film thickness was increased to ~230 nm for this study by using only 6 g of ethanol for the final dilution step of sol preparation. SEM images and 2D GISAXS pattern of titania films having 230 nm film thickness on P123 modified substrate was already reported in previous work.[46] There, it was shown that without sandwiching the films with a second modified slide, only partial orthogonal orientation was obtained. The films exhibited significant mesostructure loss even after calcination at 500 °C. Fig. 9 shows that similarly, the thicker films on modified substrates lose their long-range order quickly upon heating at elevated temperature (within 5 min at 600 °C). The intensity of the vertical (100) rod is shown in this figure, and all other long-range order was lost by the time that the final calcination temperature was reached. The normalized intensity of the (100) Bragg rod from q_z = (0.06-0.07) $Å^{-1}$ was used to generate this plot. As in the previous study,[46] more complete orthogonal alignment (in this case in thin films on modified substrates) leads to greater retention of mesostructural order during heating compared with a less completely aligned, thicker film.

The Avrami equation was applied to the mesostructure loss in thick P123-templated films on modified substrates to determine kinetic parameters. Fig. 10a shows the fitting of the Avrami equation for three isothermal conditions (400 °C, 500 °C and 600 °C because of the reduced stability of the films) of 230 nm thick P123-templated TiO_2 films on P123 modified

Physical Chemistry Chemical Physics Accepted Manuscript

substrates. The method of determination the *n* and *k* parameters was based on linear regression except for the sample at 400 °C, where the *n* value was adjusted to the average of *n* values from other two conditions and the value of *k* was calculated from the slope of a –ln(1-α) vs t^n plot using Eq. 1 (see Supporting Information Fig. S7). The reason for this adjustment is that the *n* value that was actually calculated from Fig. 10 was very low (0.29) compare to all other isothermal conditions (0.63-1.1) due to a large amount of scatter in the data due to slow deterioration. The activation energy for the mesostructural deterioration of these thick films was calculated to be 89±27 kJ/mole using an Arrhenius plot (Fig. 10b). This activation energy is clearly much lower than for both of the thin films, and lower compare to the reported activation energy of mesostructure loss of TiO_2 films with cubic mesostructures.[43] This lower activation energy suggest that preparing well-oriented, thermally stable o-HCP films by casting films onto a single substrate modified with crosslinked copolymer only works up to a certain thickness. After this critical thickness, the orthogonal orientation of pores does not propagate from the solid substrate all the way to the vapor-film interface, because of which the films form a two-layer structure consisting of orthogonal pores at the substrate-film interface and parallel pores at the vapor-film interface. Due to this mismatch of pore orientation between two layers a high density of mesostructural defects is built into the films, which aids in loss of long-range order. In addition, the mismatch of structures makes these thick films less able to withstand anisotropic stress during heating. As a result, even the orthogonal domains of thick films deteriorate very easily during heat treatment. Previous work in our group showed that sandwiching these thick films with a second modified substrate could induce orthogonal alignment throughout their thickness, thus helping the pores to withstand anisotropic stresses

Physical Chemistry Chemical Physics Accepted Manuscript

during calcination.[46] This was evident from the lower rate coefficient for mesostructure loss of 230 nm thick sandwiched films (0.047 min^{-1}) compared to unsandwiched films (0.56 min^{-1}) during calcination at 500 °C with a 25 °C/min ramp rate. This higher stability for sandwiched films rules out the possibility that the higher thermal stability found in thin films is merely a consequence of there being a smaller total force of isothermal contraction in those films. Thus, the faster loss of mesotructural order for the thick film is driven not only by the larger contraction force due curing and crystallization, but also by a lower degree of orthogonal orientation.

The above studies show that the thermal evolution of titania films at different isothermal conditions are strongly affected by the temperature history of the film. While *in situ* studies could not be performed *during* heating from room temperature due to difficulty maintaining alignment during thermal expansion, the effects of the heating rate (a.k.a. the ramp rate) on the mesophase deterioration kinetics of films calcined at 500 ° C were measured for thick films with ramp rates varying from 10 °C/min to 60 °C/min and the data were fitted using the Avrami equation *(*see Supporting Information Fig. S8). Table 3 shows the Avrami parameter values determined by linear regression for different ramp rates. For higher ramp rate, the rate coefficient (k) is found to be higher. The reason is most likely that faster heating allows the system to more quickly accumulate nuclei of crystalline material, which leads to uniform growth of titania grains and loss of mesostructural order throughout the film thickness. A greater temperature gradient at higher ramp rates may also contribute to accelerated loss of mesostructural order due to non-uniform crystallization across the film. The layer directly attached with the substrate would be expected to reach the final calcination temperature faster than the uppermost layer, resulting in faster growth of titania grains near the substrate

Physical Chemistry Chemical Physics Accepted Manuscript

than at the vapor-film interface. This kind of uneven growth of grains can introduce an anisotropic thermal stress on the pore walls that ultimately leads to faster deterioration of the mesostructure. More uniform slow heating during calcination may result in uniform growth of titania grains on the pore walls which helps to withstand anisotropic stress better than the higher ramp rates.

4. Conclusion

A detailed kinetic study of mesostructure loss in titania thin films with 2D hexagonal close packed (HCP) pores varying only in the degree and uniformity of their orthogonal orientation was conducted using *in situ* GISAXS with *ex situ* SEM imaging. Thin films (~60 nm thick) templated using P123 gave films with uniform orthogonal o-HCP orientation when the substrate was modified with crosslinked P123, and a mix of orientations (with a significant fraction of parallel pores) on unmodified glass slides. Thicker films (~230 nm thick) on modified slides also gave a mix of orientations, and prior studies suggested that had more parallel pores at the vapor-film interface and orthogonal pores at the substrate-film interface.[44]

The loss of orthogonal mesostructural order was measured using the intensity of the (100) Bragg rod from the o-HCP domains in the GISAXS patterns and analyzed using the Avrami equation. The activation energy for mesostructure deterioration was found to be greatest for the thin films on modified substrates (155±25 kJ/mole), which also had uniform o-HCP pores. A slightly smaller activation energy (128 kJ/mol) was found for thin films on unmodified substrates (with a mix of orientations) and a much smaller activation energy (89±27 kJ/mole) for thick films on modified substrates. The observed correlation of thermal stability with the degree of orthogonal orientation suggests that the density of bending defects, or the tortuosity

Physical Chemistry Chemical Physics Accepted Manuscript

of the pores associated with films on unmodified substrates makes them more susceptible to nucleation and growth of disordered regions during high temperature heating. Because thin films on modified substrate have nearly complete orthogonal orientation, they are able to withstand thermal stress during calcination without excessive mesostructure loss. This is consistent with the measured higher pre-exponential factor (suggesting a larger activation entropy) in well-ordered o-HCP films. In thick films, higher ramp rates were also found to cause more rapid mesostructure deterioration during isothermal heating. This is most likely due to nucleation of defects and formation of thermal gradients during faster heating, both of which would be expected to create stress concentrations.

These detailed kinetic results show that in addition to transport advantages of o-HCP titania films for photocatalytic and photovoltaic applications, they possess thermal and mechanical advantages over films with parallel or mixed orientation pores. The continuous pore walls normal to the film provide resistance to stress during heating, and the pore orientation provides a short diffusion path for crystallization within the walls, which both may contribute to enhanced mechanical and thermal stability for applications requiring accessible pores such as membrane separations, electrochemical sensors, and microfluidic components.

Acknowledgements

The titania thin film synthesis, characterization and GISAXS measurements were performed as part of a U.S. Department of Energy EPSCoR Implementation award supported by grant no. DE-FG02-07-ER46375. Analysis of the results was completed as part of an NSF EPSCoR research infrastructure initiative supported by grant no. IIA-1355438. The use of the Advanced Photon Source at Argonne National Laboratory for GISAXS measurements was supported by the U. S.

Physical Chemistry Chemical Physics Accepted Manuscript

Department of Energy, Office of Science, Office of Basic Energy Sciences, under Contract No. DE-AC02-06CH11357.

References

1. G. J. A. A. Soler-Illia, A. Louis and C. Sanchez, *Chem. Mater.*, 2002, 14, 750-759.
2. K. Liu, M. Zhang, K. Shi and H. Fu, *Mater. Lett.*, 2005, 59, 3308-3310.
3. E. Lancelle-Beltran, P. Prené, C. Boscher, P. Belleville, P. Buvat, S. Lambert, F. Guillet, C. Boissiere, D. Grosso and C. Sanchez, *Chem. Mater.*, 2006, 18, 6152-6156.
4. C.-T. Wang and C.-F. Yen, *Surf. Coatings Technol.*, 2012, 206, 2622-2627.
5. M. Rawolle, M. A. Niedermeier, G. Kaune, J. Perlich, P. Lellig, M. Memesa, Y.-J. Cheng, J. S. Gutmann and P. Müller-Buschbaum, *Chem. Soc.Rev.*, 2012, 41, 5131-5142.
6. R. A. Krüger, T. J. Gordon, T. Baumgartner and T. C. Sutherland, *ACS App. Mater. Interfaces*, 2011, 3, 2031-2041.
7. S. Agarwala, M. Kevin, A. Wong, C. Peh, V. Thavasi and G. Ho, *ACS App. Mater. Interfaces*, 2010, 2, 1844-1850.
8. H. Uchida, M. N. Patel, R. A. May, G. Gupta, K. J. Stevenson and K. P. Johnston, *Thin Solid Films*, 2010, 518, 3169-3176.
9. A. A. Ismail and D. W. Bahnemann, *J. Mater. Chem.*, 2011, 21, 11686-11707.
10. J. H. Pan, X. Zhao and W. I. Lee, *Chem. Eng. J.*, 2011, 170, 363-380.
11. S. Z. Islam, A. Reed, D. Y. Kim and S. E. Rankin, *Micropor. Mesopor. Mater.*, 2016, 220, 120-128.
12. P. Si, S. Ding, J. Yuan, X. W. Lou and D.-H. Kim, *ACS Nano*, 2011, 5, 7617-7626.
13. S. Hazra and S. Basu, *Sensors Actuators B: Chem.*, 2006, 115, 403-411.
14. S. R. Gajjela, K. Ananthanarayanan, C. Yap, M. Grätzel and P. Balaya, *Energy Enviro. Sci.*, 2010, 3, 838-845.
15. B. Smarsly, D. Grosso, T. Brezesinski, N. Pinna, C. Boissiere, M. Antonietti and C. Sanchez, *Chem. Mater.*, 2004, 16, 2948-2952.
16. M. Adachi, Y. Murata, J. Takao, J. Jiu, M. Sakamoto and F. Wang, *J. Am. Chem. Soc.*, 2004, 126, 14943-14949.
17. A. Rampaul, I. P. Parkin, S. A. O'Neill, J. DeSouza, A. Mills and N. Elliott, *Polyhedron*, 2003, 22, 35-44.
18. P. C. Alberius, K. L. Frindell, R. C. Hayward, E. J. Kramer, G. D. Stucky and B. F. Chmelka, *Chem. Mater.*, 2002, 14, 3284-3294.
19. E. L. Crepaldi, G. J. A. A. Soler-Illia, D. Grosso, F. Cagnol, F. Ribot and C. Sanchez, *J. Am. Chem. Soc.*, 2003, 125, 9770-9786.
20. R. Zhang, A. A. Elzatahry, S. S. Al-Deyab and D. Zhao, *Nano Today*, 2012, 7, 344-366.
21. Q. L. Wu and S. E. Rankin, *J. Phys. Chem, C*, 2011, 115, 11925-11933.
22. Q. L. Wu, N. Subramanian and S. E. Rankin, *Langmuir*, 2011, 27, 9557-9566.
23. Q. L. Wu and S. E. Rankin, *J. Sol-gel Sci. Technol.*, 2011, 60, 81-90.
24. Q. L. Wu, N. Subramanian, J. Strzalka, Z. Jiang and S. E. Rankin, *Thin Solid Films*, 2012, 520, 3558-3566.

Physical Chemistry Chemical Physics Accepted Manuscript

25. D. Grosso, G. J. A. A. Soler-Illia, F. Babonneau, C. Sanchez, P. A. Albouy, A. Brunet-Bruneau and A. R. Balkenende, *Adv. Mater.*, 2001, 13, 1085-1090.
26. S. Y. Choi, M. Mamak, N. Coombs, N. Chopra and G. A. Ozin, *Adv. Funct. Mater.*, 2004, 14, 335-344.
27. M. Zukalova, A. Zukal, L. Kavan, M. K. Nazeeruddin, P. Liska and M. Grätzel, *Nano Lett.*, 2005, 5, 1789-1792.
28. Y. Lu, R. Ganguli, C. A. Drewien, M. T. Anderson, C. J. Brinker, W. Gong, Y. Guo, H. Soyez, B. Dunn and M. H. Huang, *Nature*, 1997, 389, 364-368.
29. E. K. Richman, T. Brezesinski and S. H. Tolbert, *Nature Mater.*, 2008, 7, 712-717.
30. A. Stein, S. G. Rudisill and N. D. Petkovich, *Chem. Mater.*, 2014, 26, 259-276.
31. V. R. Koganti, D. Dunphy, V. Gowrishankar, M. D. McGehee, X. Li, J. Wang and S. E. Rankin, *Nano Lett.*, 2006, 6, 2567-2570.
32. V. R. Koganti and S. E. Rankin, *J. Phys. Chem. B*, 2005, 109, 3279-3283.
33. A. Haring, A. Morris and M. Hu, *Materials*, 2012, 5, 1890-1909.
34. K. F. Huo, B. Gao, J. J. Fu, L. Z. Zhao and P. K. Chu, *RSC Adv.*, 2014, 4, 17300-17324.
35. D. Regonini, C. R. Bowen, A. Jaroenworaluck and R. Stevens, *Mater. Sci. Eng. R-Rep.*, 2013, 74, 377-406.
36. M. Maeda and T. Watanabe, *Surf. Coatings Technol.*, 2007, 201, 9309-9312.
37. L. Malfatti, P. Falcaro, H. Amenitsch, S. Caramori, R. Argazzi, C. A. Bignozzi, S. Enzo, M. Maggini and P. Innocenzi, *Micropor. Mesopor. Mater.*, 2006, 88, 304-311.
38. A. Alem, H. Sarpoolaky and M. Keshmiri, *Ceram. Internat.*, 2009, 35, 1837-1843.
39. D. Grosso, G. J. A. A. Soler-Illia, E. L. Crepaldi, F. Cagnol, C. Sinturel, A. Bourgeois, A. Brunet-Bruneau, H. Amenitsch, P. A. Albouy and C. Sanchez, *Chem. Mater.*, 2003, 15, 4562-4570.
40. P. Yang, D. Zhao, D. I. Margolese, B. F. Chmelka and G. D. Stucky, *Nature*, 1998, 396, 152-155.
41. K. Cassiers, T. Linssen, M. Mathieu, Y. Q. Bai, H. Y. Zhu, P. Cool and E. F. Vansant, *J. Phys. Chem. B*, 2004, 108, 3713-3721.
42. K. Wang, M. A. Morris and J. D. Holmes, *Chem. Mater.*, 2005, 17, 1269-1271.
43. B. L. Kirsch, E. K. Richman, A. E. Riley and S. H. Tolbert, *J. Phys. Chem. B*, 2004, 108, 12698-12706.
44. J. D. Bass, D. Grosso, C. Boissiere and C. Sanchez, *J. Am. Chem. Soc.*, 2008, 130, 7882-7897.
45. M. A. Carreon, S. Y. Choi, M. Mamak, N. Chopra and G. A. Ozin, *J. Mater. Chem.*, 2007, 17, 82-89.
46. S. Das, Q. Wu, R. K. Garlapalli, S. Nagpure, J. Strzalka, Z. Jiang and S. E. Rankin, *J. Phys. Chem. C*, 2014, 118, 968-976.
47. I. Arabatzis, T. Stergiopoulos, M. Bernard, D. Labou, S. Neophytides and P. Falaras, *Appl. Catal. B: Enviro.*, 2003, 42, 187-201.
48. W.-L. Chang, H.-W. Su and W.-C. Chen, *Eur. Polym. J.*, 2009, 45, 2749-2759.
49. Z. Jiang, X. Li, J. Strzalka, M. Sprung, T. Sun, A. R. Sandy, S. Narayanan, D. Lee and J. Wang, *J. Synchrotron Rad.*, 2012, 19, 627-636.
50. Z. Jiang, *J. Appl. Cryst.*, 2015, 48, 917-926.
51. S. Nagpure, S. Das, R. K. Garlapalli, J. W. Strzalka and S. E. Rankin, *J. Phys. Chem. C*, 2015.

Physical Chemistry Chemical Physics Accepted Manuscript

52. M. Klotz, P.-A. Albouy, A. Ayral, C. Ménager, D. Grosso, A. Van der Lee, V. Cabuil, F. Babonneau and C. Guizard, *Chem. Mater,*, 2000, 12, 1721-1728.
53. J. Augis and J. Bennett, *J. Therm. Anal. Calorim.*, 1978, 13, 283-292.
54. W. Banks and A. Sharples, *Makromol. Chem.*, 1963, 59, 233-236.
55. Z. Ding and J. E. Spruiell, *J. Polym. Sci. B: Polym. Phys.*, 1997, 35, 1077-1093.
56. J. F. Toro-Vazquez, E. Dibildox-Alvarado, M. Charó-Alonso, V. Herrera-Coronado and C. A. Gómez-Aldapa, *J. Am. Oil Chem. Soc.*, 2002, 79, 855-866.

Physical Chemistry Chemical Physics Accepted Manuscript

Table 1 Avrami parameters *n* and *k* determined using the linearized Avrami equation at different isothermal conditions for titania thin films (60 nm thick) on both unmodified and modified borosilicate glass substrates.

Substrate	Temp (°C)	*n*	*k* (min^{-1})
Unmodified	600	0.7±0.09	0.063±0.02
	625	0.75±0.19	0.054±0.04
	650	1.1±0.05	0.164±0.02
Modified	600	0.81±0.06	0.023±0.004
	625	0.82±0.06	0.049±0.004
	650	0.63±0.22	0.073±0.038

Table 2 Avrami parameters *n* and *k* determined using the linearized Avrami equation at different isothermal conditions for titania thick films (250 nm thick) on modified substrate.

Temp (°C)	*n*	*k* (min^{-1})
400	0.89±.09	0.009±0.002
500	0.9±.06	0.178±0.02
600	0.88±1.2	0.322±0.24

Table 3 Avrami parameters *n* and *k* determined using the linearized Avrami equation for different ramp rates to reach the final calcination temperature of 500 °C for titania thick films (250 nm thick) on modified substrate.

Ramp rate (°C/min)	*n*	*k* (min^{-1})
10	0.72±0.14	0.233±0.044
25	0.9±0.06	0.178±0.014
30	0.67±0.06	0.243±0.032
40	0.62±0.09	0.64±0.154
60	0.67±0.03	0.444±0.042

Physical Chemistry Chemical Physics Accepted Manuscript

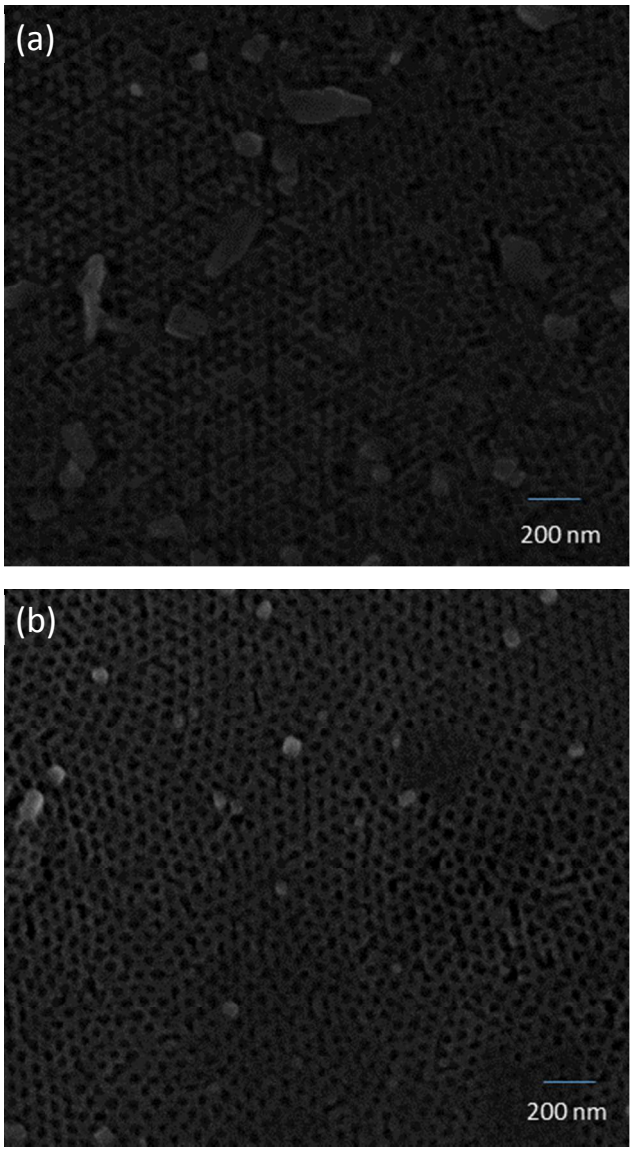

Fig. 1 SEM images of the top surface of thin titania films (~60 nm thick) on (a) unmodified (b) modified borosilicate glass slides aged for 2 h at 4 °C and immediately calcined at 500 °C for 60 min after heating at a rate of 40 °C/min.

Physical Chemistry Chemical Physics Accepted Manuscript

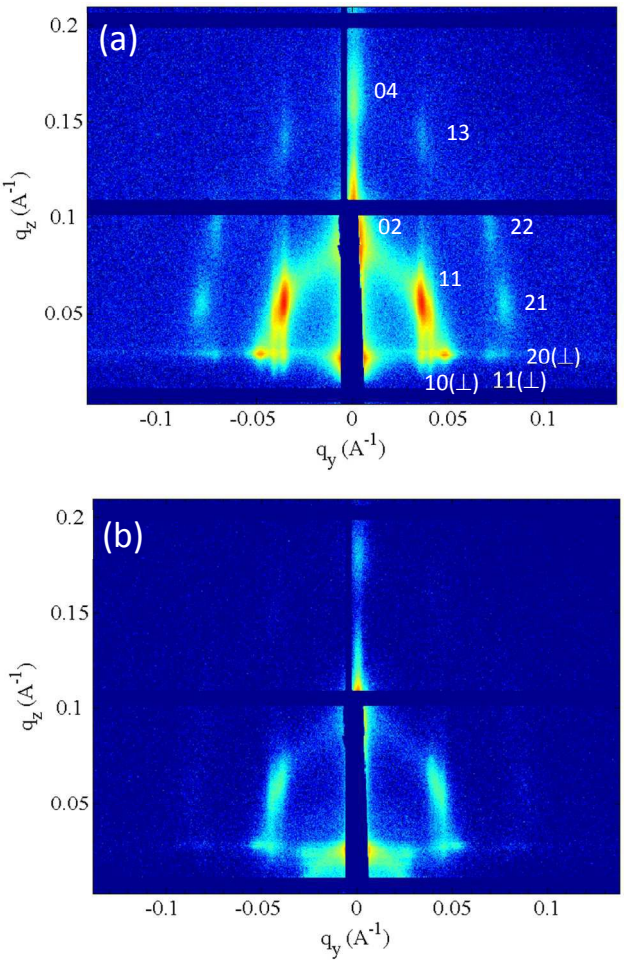

Fig. 2 GISAXS patterns at room temperature (22.5 °C) of titania thin films (60 nm thick) on (a) unmodified and (b) modified substrate after aging at 4 °C for 2 h but before calcination. The films are oriented horizontally (in the xy plane) relative to the incident beam for this experiment. In part (a), spots are indexed to combination a rectangular phase (C2mm spacegroup) oriented parallel to the substrate and an o-HCP phase (indicated with ⊥).

Physical Chemistry Chemical Physics Accepted Manuscript

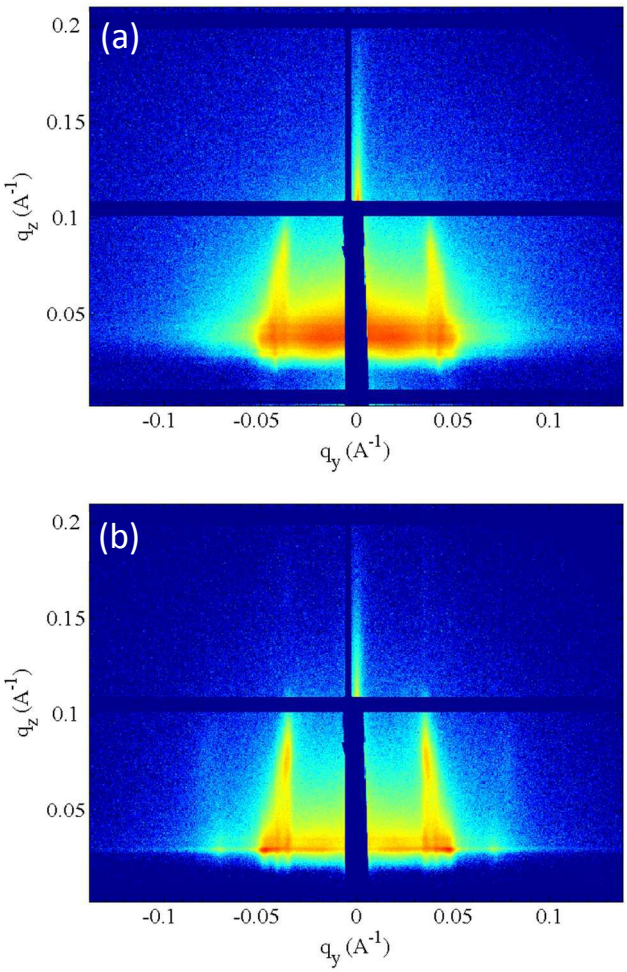

Fig. 3 GISAXS patterns of titania thin films (60 nm thick) on (a) unmodified and (b) modified substrate after aging at 4 °C for 2 h and just after reaching final calcination temperature 600 °C with a 40 °C/min ramp rate. The films are oriented horizontally (in the xy plane) relative to the incident beam for this experiment.

Physical Chemistry Chemical Physics Accepted Manuscript

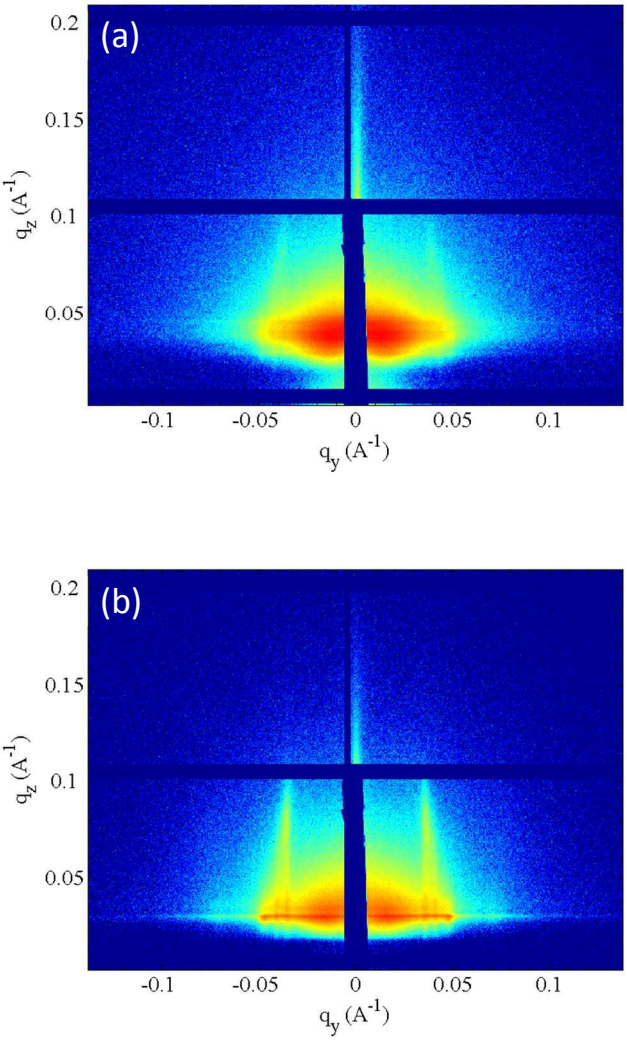

Fig. 4 GISAXS pattern of titania thin films (60 nm thick) on (a) unmodified and (b) modified substrate after heating at 40 °C/min to 600 °C and holding at that temperature for 60 min. The film is oriented horizontally (in the xy plane) relative to the incident beam for this experiment.

Physical Chemistry Chemical Physics Accepted Manuscript

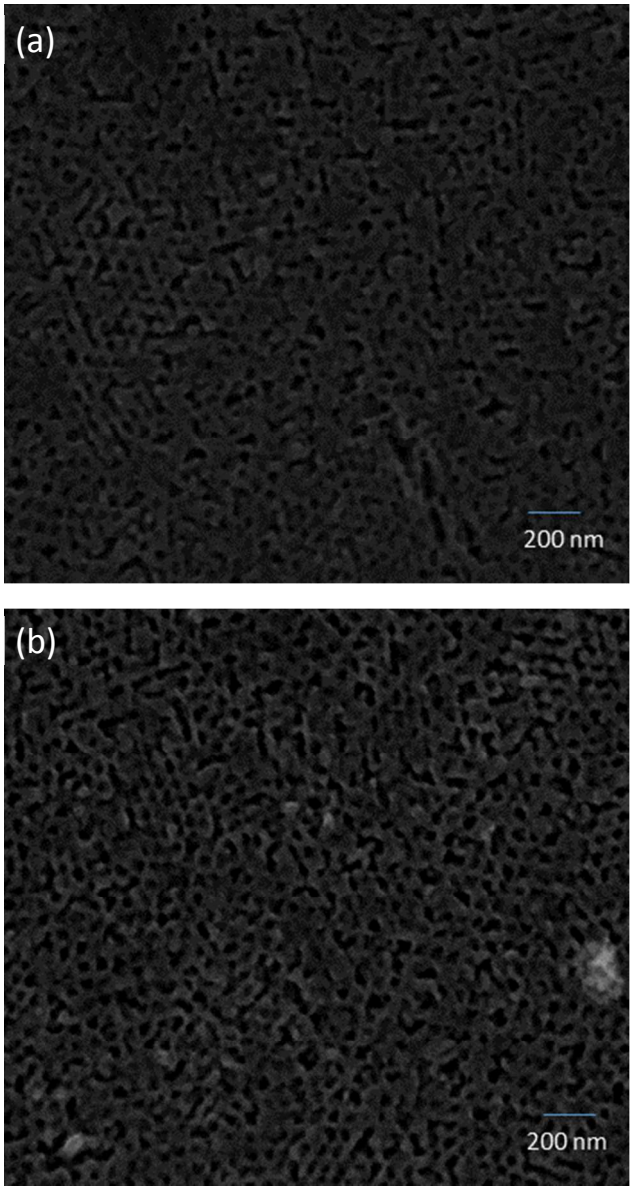

Fig. 5 SEM images of titania films on (a) unmodified (b) modified substrate aged at 4 °C for 2 h and calcined at 600 °C for (a) 60 min and (b) 90 min after heating at a rate of 40 °C/min.

Physical Chemistry Chemical Physics Accepted Manuscript

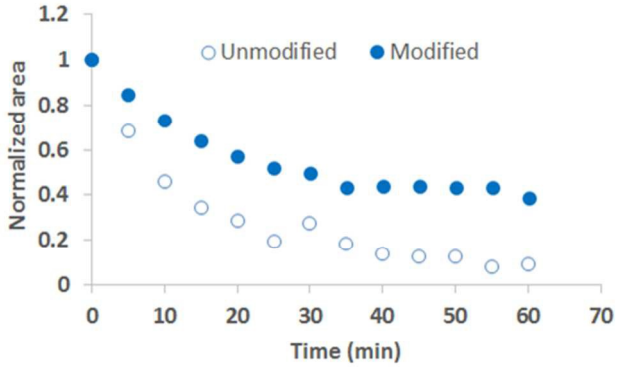

Fig. 6 Normalized (100) diffraction peak height measured from line cuts over q_z values from 0.06-0.07 $Å^{-1}$ from *in situ* GISXAS data for titania thins films during isothermal treatment at 600 °C after heating at a ramp of 40 °C/min.

Physical Chemistry Chemical Physics Accepted Manuscript

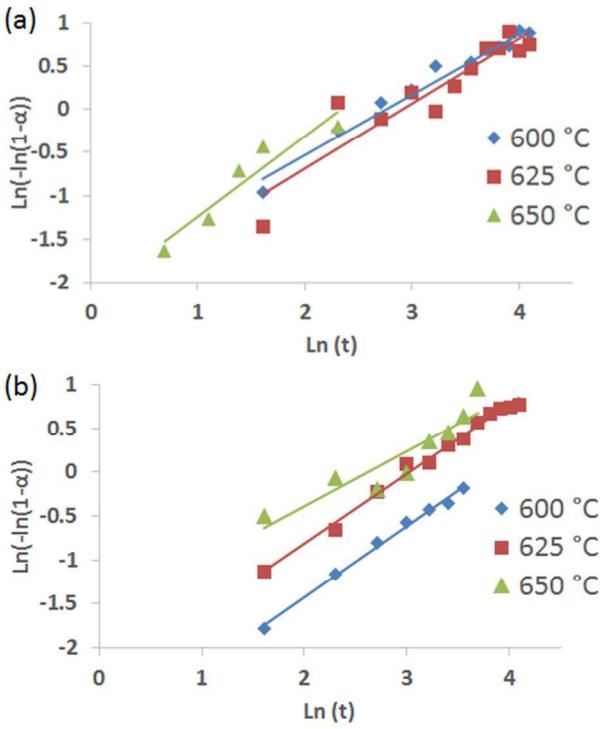

Fig. 7 Avrami equation plots based on (100) peak intensity data for thin titania films (~60 nm thick) on (a) unmodified and (b) modified substrates at different isothermal conditions after ramping at 40 °C/min.

Physical Chemistry Chemical Physics Accepted Manuscript

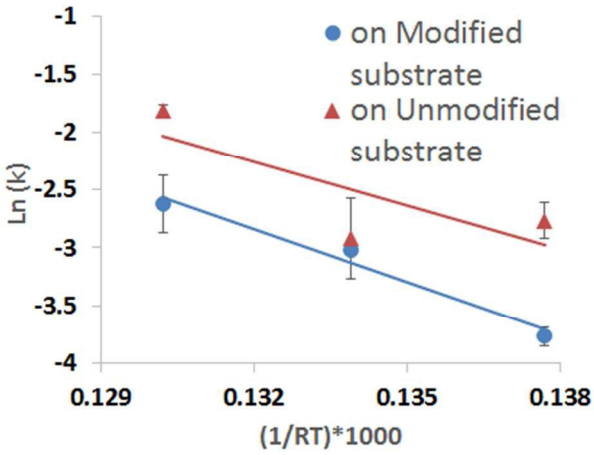

Fig. 8 Arrhenius plot for HCP mesostructure loss of thin (~60 nm thick) titania films on modified and unmodified borosilicate glass substrates.

Physical Chemistry Chemical Physics Accepted Manuscript

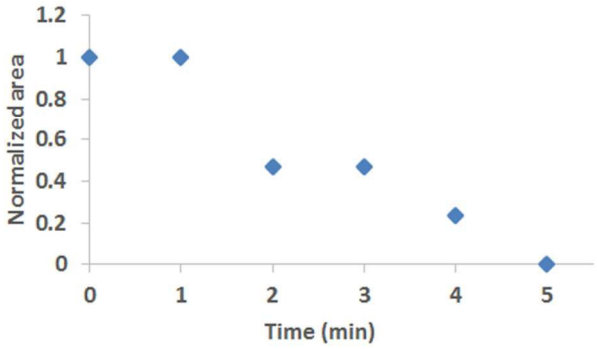

Fig. 9 Evolution of the normalized (100) diffraction peak height from linecuts taken over q_z from 0.06-0.07 $Å^{-1}$ from *in situ* GISXAS data of titania thick films (~250 nm thick) on modified borosilicate glass slides during isothermal treatment at 600 °C after heating at 25 °C/min.

Physical Chemistry Chemical Physics Accepted Manuscript

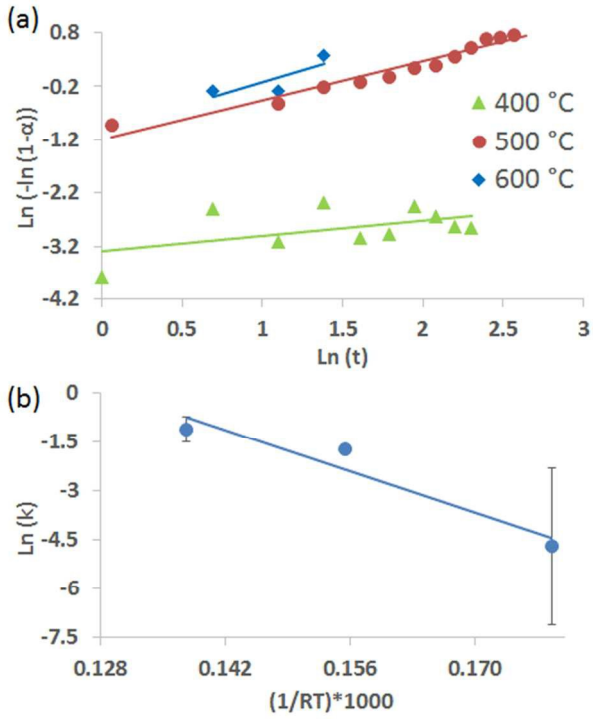

Fig. 10 Plot of the (a) linearized Avrami equation and (b) Arrhenius equation fits for thick (~250 nm) titania films on modified borosilicate glass slides at different isothermal conditions after heating at a ramp rate of 25 °C/min.

Physical Chemistry Chemical Physics Accepted Manuscript